Colloidal suspensions at dielectric interfaces

2000 J. Phys.: Condens. Matter 12 10349

(http://iopscience.iop.org/0953-8984/12/50/301)

J. Phys.: Condens. Matter **12** (2000) 10349–10370. Printed in the UK PII: S0953-8984(00)16708-6

Colloidal suspensions at dielectric interfaces

H H von Grünberg and E C Mbamala
Fakultät für Physik, Universität Konstanz, 78457 Konstanz, Germany

Received 30 August 2000

Abstract. We study suspensions of charged mesoscopic spheres (colloids) near typical dielectric interfaces. Having a dielectric constant that is different from that of the suspension, the interface gives rise to image-charge-induced forces which compete with the usual double-layer forces acting between the colloids. Within the framework of Poisson–Boltzmann theory we calculate the total force acting on an interfacial macrosphere for a broad range of possible system parameters. These are: the ratio of dielectric constants of the two media, the charge and size of the macroion, its distance from the wall, the temperature and volume fraction of the suspension. To reduce the number of parameters, use is made of the scaling property of the Poisson–Boltzmann equation in the salt-free approximation. We have furthermore performed Monte Carlo simulations to investigate finite-size effects of the microions. We discuss, quite generally, how both confinement effects and image charges affect the structural properties of interfacial colloidal suspensions and explain how our results can be used for estimating their effects in experiments.

1. Introduction

The interaction of many important biomolecules in solution, among them such prominent examples as the DNA molecule, is dominated by the electric double layer that forms around the charged molecules when they are suspended in a polar solvent. A particularly simple model system that lends itself well to the study of these double-layer interactions is a suspension of highly charged spheres (mesoscopic in size) in a microionic fluid (realized, for instance, by an aqueous latex suspension). While, in bulk, this example of a charge-stabilized colloidal suspension has been the subject of a vast number of theoretical investigations [1], there are only very few studies of the structural properties of interfacial colloidal suspensions [2–5], and of them, an even smaller number take proper account of image charges to simulate the effect of the dielectric discontinuity at the interface [3–5].

This is the more surprising since this simple suspension is again well suited as a model system to study, in general, the basic effects of image charges on the structural properties of a suspension of charged objects, be it an ion near a protein or a single DNA molecule (carrying a large charge) near a membrane [6]. With respect to membrane/electrolyte systems, only a few studies exist that have addressed the question of image-charge effects [7, 8]. But also concerning the ongoing debate [2, 3] about the unexpected findings of attractive interaction between colloids near and between planar glass walls [9] and at the air–water interface [10], a clear understanding of the role played by image charges is a necessary prerequisite for coming to any consistent interpretation of the experimental data. Other examples for the significance of image charges are the problem of aggregation [11], melting [12], structural ordering of colloidal dispersions near walls [5, 13, 14], and even the question of the effective colloid/colloid interaction in bulk [15].

0953-8984/00/5010349+22$30.00

The bulk behaviour of macroionic suspensions is expected to change significantly in the presence of neutral or charged dielectric interfaces in contact with, or confining the dispersion, such as electrodes, container walls, and air. The present article addresses the question of what effect such a dielectric interface will have on the structure of a concentrated suspension of charged colloids. In particular, we want to know whether a colloid (or macroion, which we use as synonym for the word 'colloid') near the interface experiences additional image-charge-induced forces, and if so, how strong these are. We do not have a particular interface in mind, but aim to discuss—in as general terms as possible—the effect solely of the dielectric discontinuity on the colloid. The interface therefore is thought of as a planar, structureless, uncharged wall confining the colloidal suspension. Its dielectric constant, ϵ', is different from the dielectric constant ϵ of the solvent.

To demonstrate that the guiding question of this article has no trivial answer, we briefly mention the various aspects of the problem. First, the wall is not penetrable, neither for the colloid nor for electrolyte ions. This results in a pure confinement effect which arises from the distortion of the ionic atmosphere around each interfacial colloid. Secondly, the dielectric discontinuity across the interface will lead to additional external fields felt by all ions near the wall (macroions and microions). And, third, any interfacial colloid will still interact with all other colloidal particles in the solution plus their surrounding ions. We will see that the combination of the last two factors leads to an attractive net force on the interfacial colloid for all ratios ϵ'/ϵ between zero and one, while the confinement effect leads to repulsion. The question thus is that of which effect prevails and at what wall–particle distance and whether or not these forces will be strong enough to cause any significant structural rearrangement of the colloidal suspension near the wall. We will answer this question with the help of a Poisson–Boltzmann (PB) cell theory and Monte Carlo (MC) simulations.

There are a number of works concerned with image-charge effects in pure electrolyte solutions, a problem that is closely related to ours. An electrolyte close to a charged planar wall has been the subject of MC simulations by Torrie *et al* [16] and by Bratko *et al* [17]. A similar system has also been investigated by Kjellander and Marcelja [18] on a hypernetted-chain level, as well as by Levine and Outhwaite [19] who have done similar work within the framework of the PB theory. Linse [20], employing the same concept (image charge), performed a MC simulation in the cell model approximation [21, 22] to investigate the effect of image charges on the properties of a spherical electric double layer for a micellar model system. Several papers can be found where the Debye–Hückel theory, based on the linearized PB equation, has been generalized to interfacial geometries [23–25].

This article is divided into two main sections: section 2 where we introduce our PB cell model, discuss the resulting boundary-value problem and present our PB results; and section 3 which is devoted to the presentation of the MC data.

2. Poisson–Boltzmann theory

2.1. The interfacial Poisson–Boltzmann cell model

We model the charge-stabilized colloidal suspension by mesoscopic, charged spheres that are suspended in a solvent and surrounded by microions. We assume that there is a finite concentration n_m of these spherical macroions, so the volume per macroion is $V_{WS} = 1/n_m$ (this is equal to the Wigner–Seitz (WS) cell volume in the crystalline phase). The macroion has a radius a and fills a volume $V_m = 4\pi a^3/3$. Each bears Z positive charges and thus produces the same number of singly charged, negative, point-like counterions, whose concentration then is $c_0 = Z/\tilde{V}_{WS}$ with $\tilde{V}_{WS}$ being the part of the WS cell volume that is not already occupied by

the macroion, $\tilde{V}_{WS} = V_{WS} - V_m$. In addition, there are usually other microions (salt) present in the suspension, but, for reasons that soon become obvious, we here assume that their number per cell is much smaller than the number of counterions. This approximation is good for highly de-ionized solutions and/or for suspensions of sufficiently high concentration.

The forces between the macroions are determined by the (inhomogeneous) distribution of the microionic fluid between them. On a mean-field level of description, this distribution of the mobile microions can be calculated from the PB equation [26]. Though being originally designed for the case of isolated charged objects in an ionic solution, the PB theory applies equally well to concentrated suspensions of charged colloids, provided that the cage of neighbouring macroions is modelled by a cell of finite volume, to which the macroion is confined. The entire problem of finding the density distribution then reduces to solving the PB equation inside a single cell only. Such PB cell models are useful because they allow conversion of the whole problem into one well-defined boundary-value problem (BVP), and have been used repeatedly not only for describing bulk colloidal suspensions [27–33], but also for PB theories for swollen clay [34] and polyelectrolytes [22, 35].

The basic assumption of these cell models is that every colloidal particle of the suspension experiences the same environment, which we know is strictly true only for the crystalline phase. So, in a bulk suspension, each macroion is assumed to be located at the centre of its cell, and all cells of the suspension have the same volume and shape. The presence of the other particles of the suspension is taken into account by the appropriate choice of the boundary conditions. These conditions plus the PB equation then constitutes a BVP whose solution provides us with a mean electrostatic potential and thus a microionic density distribution. From it, one can then derive general thermodynamic quantities of the suspension, such as the osmotic pressure [28], or more specific quantities, such as the effective pair forces between the particles [32].

Considering in this article a suspension that borders a dielectric interface, we here suggest a cell model that is adapted to the interfacial geometry (figure 1). The WS cell of a colloidal particle near to a dielectric interface is now assumed to have the shape of a cylinder of radius r_0 and length z_1 (the z-axis is perpendicular to the wall, with $z = 0$ defining the interface). r_0 is given by the volume of the WS cell, $V_{WS} = \pi r_0^2 z_1$, with the additional assumption that the cell has the same aspect ratio as a cube, $z_1 = 2r_0$†. The macroion inside this cell is situated at $z = z_0$ and $r = 0$. At $z = 0$, the dielectric constant of the medium changes from ϵ' to ϵ. At $z < 0$, there are no real charges.

Inside this interfacial cell, we solve the PB equation which in our salt-free case reads

$$\nabla^2 \Phi(\vec{r}) = 4\pi \lambda_B \rho(\vec{r}) \tag{1}$$

with a charge density $\rho(\vec{r})$ that depends on $\Phi = e\beta\Psi$, the normalized mean electrostatic potential, in the following way:

$$\rho(r, z) = c_0 \mathrm{e}^{\Phi(r,z)} \Theta(R(r, z) - a) + \rho_m(r, z). \tag{2}$$

$\lambda_B = e^2\beta/\epsilon$ is the Bjerrum length, and $\beta = 1/k_B T$ the inverse temperature. The charge distribution $\rho(\vec{r})$, equation (2), is given in units of $-e$ and consists of two terms of which the first is the contribution of the microions in the region exterior to the colloid. This is ensured by the Θ step function, which changes from zero to one when its argument becomes greater than zero. R measures the radial distance of a point inside the cylinder to the centre, $R^2 = r^2 + (z - z_0)^2$. The second term in equation (2), ρ_m, is the charge distribution of the colloid, whose charges are usually assumed to be homogeneously smeared out over the

† This additional approximation is not necessary. One can allow for two independent parameters, z_1 and r_0, and then find the optimal aspect ratio from minimizing the total free energy per cell with respect to the aspect radius. We checked the sensitivity of our results to the aspect ratio, and found only a very weak dependence on it.

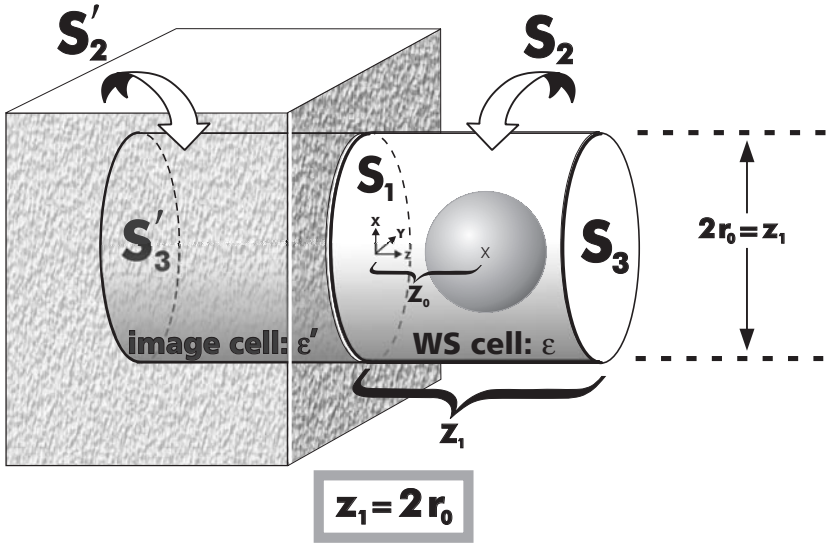

Figure 1. The interfacial cell model: a colloid of charge Ze is located at a position z_0 inside a cylindrical Wigner–Seitz (WS) cell of length z_1 and radius r_0 with $2r_0 = z_1$. This cell is filled with Z counterions and confined by three surfaces S_1, S_2, and S_3, of which S_1 is a dielectric interface where the dielectric constant of the medium changes from ϵ to ϵ'. In the ϵ'-medium, there is the mirror image of the original cell, the image cell, with the confining surfaces S_1, S_2', and S_3'.

colloidal surface. To reduce grid errors in our numerical procedure, we however take them to be homogeneously distributed in a thin spherical shell near to the colloidal surface. This shell is defined by the two radii b and a ($b < a$, $a - b \ll a$). The colloidal charge density then reads

$$\rho_m = -\frac{3Z\Theta(a-R)\Theta(R-b)}{4\pi(a^3-b^3)} \tag{3}$$

and is, of course, not dependent on the electrostatic potential.

In order to be able to set up a BVP, we have to specify the boundary conditions for our cell model. Let us call the three confining surfaces of the cell S_1, S_2, and S_3, the first one being the interface to the dielectric medium, the second one the surface of the cylinder, and the last one the surface directed towards the bulk suspension (see figure 1). If for the moment we assume the colloidal particle to be located at the centre of the cell, $z_0 = 0.5z_1$, then the boundary conditions at S_2 and S_3 follow from the assumption that the corresponding surfaces lie sufficiently near to the mid-planes between two neighbouring colloids where, for symmetry reasons, the electric fields exactly cancel each other. The third boundary condition at S_1 comes from the requirement that the jump in the normal component of the electric displacement field across the interface must be equal to the surface charge density $-e\sigma$ at the interface. Collecting the pieces together now, we obtain the following BVP:

$$\begin{aligned}
&\left(\partial_r^2 + \frac{1}{r}\,\partial_r + \partial_z^2\right)\Phi(r,z) = 4\pi\lambda_B\left(c_0 \mathrm{e}^{\Phi(r,z)}\Theta(R-a) + \rho_m(r,z)\right)\\
&S_1: \qquad \epsilon\,\partial_z\Phi\big|_{z=0+} = \epsilon'\,\partial_z\Phi\big|_{z=0-} + 4\pi e^2\beta\sigma\\
&S_2: \qquad \partial_r\Phi = 0\\
&S_3: \qquad \partial_z\Phi = 0.
\end{aligned} \tag{4}$$

In addition, we have to require that (i) the potential is continuous across the interface and that

(ii) each WS cell must be electrically neutral. We therefore choose the additive constant of Φ such that

$$c_0 \int_{\tilde{V}_{WS}} \mathrm{e}^{\Phi}\, \mathrm{d}V = Z + \Sigma. \tag{5}$$

Then the total number of counterions in a cell equals the sum of the colloidal charge number plus the interfacial charge number, $\Sigma = \sigma\pi r_0^2$.

Equation (4) can be brought into a more convenient form by introducing reduced units. A good candidate as a unit length is the radius a of the colloid which in the following we take to be one. Recalling that $c_0 = Z/\tilde{V}_{WS}$ and realizing that

$$\tilde{V}_{WS} = V_m \frac{1-\phi_{vol}}{\phi_{vol}} \tag{6}$$

with $\phi_{vol} = V_m/V_{WS}$ being the volume fraction and $V_m = 4\pi/3$ the volume of the colloidal particle, we rewrite equation (4) using equations (3) and (6) as

$$\left(\partial_r^2 + \frac{1}{r}\,\partial_r + \partial_z^2\right)\Phi(r,z) = 3\tilde{\lambda}_B Z\left(\frac{\phi_{vol}}{1-\phi_{vol}}\mathrm{e}^{\Phi(r,z)}\Theta(R-1) - \frac{\Theta(1-R)\Theta(R-b)}{1-b^3}\right)$$

$$S_1: \qquad \partial_z\Phi\big|_{z=0+} = \frac{\epsilon'}{\epsilon}\,\partial_z\Phi\big|_{z=0-} + 4\pi\tilde{\lambda}_B\tilde{\sigma} \tag{7}$$

$$S_2: \qquad \partial_r\Phi = 0$$

$$S_3: \qquad \partial_z\Phi = 0.$$

The tilde over $\tilde{\lambda}_B$ is to remind us that the Bjerrum length has to be given in units of a now. For the same reason we write $\tilde{\sigma} = \sigma a^2$. From equation (7), one can recognize that the whole calculation needs four independent input parameters, which are the volume fraction ϕ_{vol}, the ratio of dielectric constants ϵ'/ϵ, the scaled colloidal charge $Z\tilde{\lambda}_B$, and the scaled interfacial surface charge $\tilde{\sigma}\tilde{\lambda}_B$. The parameter b ($b < 1$) also appearing in equation (7), has been introduced for technical reasons only. We have made sure that it does not affect our results.

That the problem can be reduced to just four independent parameters, is owed to the fact that the PB equation in the salt-free case scales with $Z\lambda_B/a$, an observation first made by Groot [29]. This scaling property is lost when salt ions are present which is the main reason for our considering the salt-free limit. It enables us to study the problem in the widest possible sense by working through these four parameters only. However, since our main concern in this article is the study of image-charge effects on colloidal particles, we concentrate on cases where $\sigma = 0$.

In a purely electrostatic problem, the complicated boundary condition at S_1 in equation (7) is satisfied by means of the well-known image-charge method, where every ion of charge q in the neighbourhood of the dielectric wall has an image charge of a magnitude $q\eta$ with

$$\eta = \frac{\epsilon - \epsilon'}{\epsilon + \epsilon'} \tag{8}$$

in the half-space where $z < 0$. We know that in most experimentally relevant cases, ϵ is much larger than ϵ' (water: $\epsilon = 78$; air: $\epsilon' = 1.0$; quartz, SiO_2: $\epsilon' = 4.5$; micas: $\epsilon' = 5.4$). It should therefore suffice to investigate ratios ϵ'/ϵ between zero and one only, so that η varies between $\eta = 1$ (for $\epsilon'/\epsilon = 0$) and $\eta = 0$ (for $\epsilon'/\epsilon = 1$). That means that the image charges for $\epsilon'/\epsilon = 0$ will have the same sign and the same magnitude as the original charges, while they will be non-existent when $\epsilon'/\epsilon = 1$. In the appendix, we explain why this method cannot be applied straightforwardly to a PB problem. We therefore solve equation (7) by an iterative procedure explained below and use the image-charge concept in our MC simulations only. We nevertheless will repeatedly refer to image charges in the discussion of our PB results

because image charges are not only a powerful technical concept, but also useful for picturing the effects arising from the dielectric discontinuity.

Note that the BVP of equation (7) leads back to a bulk cell problem, if we choose $\sigma = 0$ and $\epsilon' = 0$. For then, the electric fields on all three sides are the same in accordance with the symmetry requirement in a bulk situation. The only difference from the standard PB cell model [28] then remains the cylindrical shape of the cell as opposed to the spherical cell usually assumed; but as regards the density profiles, this difference has proven to be insignificant. At first, one might think that a choice $\epsilon' = \epsilon$ should give the bulk situation; but from equation (8), we know that $\epsilon' = 0$ means that the image charges are fully switched on ($\eta = 1$). The ion distribution in the cell at $z > 0$ thus has a perfect mirror image at $z < 0$. The latter then simulates the density distribution in a next-neighbour cell in bulk. Hence, for symmetry reasons, the normal component of the electric field must vanish at $z = 0$. The bulk situation is thus recovered.

Finally, we note that the surface of the colloidal particle defines another interface where the dielectric constant changes. This will lead to image charges inside the colloid which we have not taken into account here, but which in an anisotropic situation like ours can have an effect as well.

2.2. The iterative procedure for the matching condition

Equation (7) as it stands can only be solved in the special case where $\epsilon' = 0$ because only then does one have clearly defined boundary conditions at all three confining surfaces of the cell. If $\epsilon' \neq 0$, then the condition at S_1 constitutes, strictly speaking, a matching condition rather than a boundary condition. It links the potential at $z > 0$ to the potential at $z < 0$ which is a solution to the Laplace equation. We now explain an iterative procedure by means of which these two solutions can be linked together.

To calculate the potential at $z < 0$ we construct an image cell in the negative half-space ($z < 0$) where the dielectric constant is ϵ' (see figure 1). It is the mirror image of the original interfacial cell at $z > 0$. Its confining surfaces are S_1, S_2', and S_3'. There are no real charges in this cell, so the problem to solve is

$$\begin{aligned} &\left(\partial_r^2 + \frac{1}{r}\,\partial_r + \partial_z^2\right)\Phi(r,z) = 0 \\ &S_1: \qquad \Phi\big|_{z=0} = v(r) \\ &S_2': \qquad \partial_r \Phi = 0 \\ &S_3': \qquad \partial_z \Phi = 0 \end{aligned} \tag{9}$$

with a potential $v(r)$ at S_1 that we soon specify. Equation (9) has the following solution:

$$\Phi(r,z) = \sum_{m=1}^{\infty} A_m J_0\left(y_{0m}\frac{r}{r_0}\right)\cosh\left(y_{0m}\frac{z+z_1}{r_0}\right) \tag{10}$$

where the coefficients A_m are given by

$$A_m = 2\left(\cosh\left(y_{0m}\frac{z_1}{r_0}\right)r_0^2 J_0^2(y_{0m})\right)^{-1}\int_0^{r_0} v(x)\,x\,J_0\left(y_{0m}\frac{x}{r_0}\right)\mathrm{d}x. \tag{11}$$

In these expressions, J_0 and J_1 are the usual Bessel functions and y_{0m} is the mth root of the function J_1. The derivative of equation (10) at $z = 0$ is

$$\partial_z \Phi(r,0) = \sum_{m=1}^{\infty} B_m J_0\left(y_{0m}\frac{r}{r_0}\right)\int_0^{r_0} v(x)\,x\,J_0\left(y_{0m}\frac{x}{r_0}\right)\mathrm{d}x \tag{12}$$

with

$$B_m = \tanh\left(y_{0m}\frac{z_1}{r_0}\right)\frac{2y_{0m}}{r_0^3 J_0^2(y_{0m})}. \tag{13}$$

With equations (9) to (13) to hand, we can now give an iterative scheme to solve equation (7). Let us call $\Phi^{(n)}$ the potential in the nth iteration cycle. From equation (7), we see that in order to be able to calculate that potential we need to know $\partial_z \Phi^{(n)}\big|_{z=0+}$, which we can now obtain from equation (12). This expression in turn is based on the knowledge of the potential at $z = 0$, that is on $v(r)$, for which we take the potential from the previous iteration step, $\Phi^{(n-1)}$. To cast this idea into a mathematical form, we rewrite equation (7) once more and find

$$\left(\partial_r^2 + \frac{1}{r}\,\partial_r + \partial_z^2\right)\Phi^{(n)}(r,z) = 3\tilde{\lambda}_B Z\left(\frac{\phi_{vol}}{1-\phi_{vol}}\mathrm{e}^{\Phi^{(n)}(r,z)}\Theta(R-1) - \frac{\Theta(1-R)\Theta(R-b)}{1-b^3}\right)$$

$$S_1: \qquad \partial_z \Phi^{(n)}\big|_{z=0+} = \frac{\epsilon'}{\epsilon}\left(\sum_{m=1}^{\infty} B_m J_0\left(y_{0m}\frac{r}{r_0}\right)\int_0^{r_0}\Phi^{(n-1)}(x,0)\,x\,J_0\left(y_{0m}\frac{x}{r_0}\right)\mathrm{d}x\right) + 4\pi\tilde{\lambda}_B\tilde{\sigma} \tag{14}$$

$$S_2: \qquad \partial_r \Phi^{(n)} = 0$$

$$S_3: \qquad \partial_z \Phi^{(n)} = 0$$

plus the condition

$$c_0 \int_{\tilde{V}_{WS}} \mathrm{e}^{\Phi^{(n)}}\,\mathrm{d}V = Z + \Sigma \tag{15}$$

for the choice of the additive constant of $\Phi^{(n)}$. The coefficients B_m appearing in equation (14) are to be taken from equation (13). This iterative scheme ensures that (i) the potential is continuous across the interface, (ii) the normal component of the electric displacement field changes in the correct way, and (iii) the additive constant of the potential is chosen in accordance with the electro-neutrality condition. As an initial value for the potential one can take the solution of equation (7) for $\epsilon' = 0$. In practice, one varies the ratio ϵ'/ϵ starting from $\epsilon'/\epsilon = 0$ and takes the solution for a given value of this ratio as an initial guess for the next higher value.

Given the solution Φ from equation (14), we can now calculate the force acting on the colloid. Clearly, it is directed in the z-direction and we abbreviate its z-component as F_z. It can be obtained by integrating the stress tensor $\vec{\vec{T}}$:

$$\vec{\vec{T}} = \left(\Pi + \frac{\epsilon}{8\pi}E^2\right)\vec{\vec{I}} - \frac{\epsilon}{4\pi}\vec{E}\vec{E} \tag{16}$$

(Π is the local osmotic pressure, $\vec{E}$ the electric field) over a surface S enclosing the colloidal particle:

$$F_z = \int_S \mathrm{d}S\,\vec{n}\cdot\vec{\vec{T}}\cdot\vec{e}_z. \tag{17}$$

$\vec{n}$ is a unit vector directed normal to the surface S (inward direction); $\vec{e}_z$ is a unit vector in the positive z-direction. A natural choice for the enclosing surface are the three surfaces confining our cell, i.e. S_1, S_2, and S_3. At S_2, we know from equation (14) that the electric field component normal to the surface is zero, so the tensor element T_{rz} vanishes. Then, evaluation of equation (17) shows that the force takes a particularly simple form:

$$\gamma F_z = \gamma F(0) - \gamma F(z_1) \tag{18}$$

with $\gamma = 4\lambda_B\beta$ and

$$\gamma F(z) = \int_0^{r_0} \left[\frac{6\tilde{\lambda}_B Z \phi_{vol}}{1-\phi_{vol}} \mathrm{e}^{\Phi(r',z)} + \left(\partial_{r'}\Phi(r',z)^2 - \partial_z \Phi(r',z)^2 \right) \right] r' \, \mathrm{d}r'. \quad (19)$$

Note that the force is given in the usual dimensionless form. The first term in equation (19) is due to the local osmotic pressure while the second accounts for the stress induced by the electric field. It is advisable to check the function $\gamma F(z)$ because it is of great help for monitoring the accuracy of the calculation. Ideally it should be a horizontal line for all $z < z_0 - 1$ and a different, but again horizontal line for all $z > z_0 + 1$, i.e., to the left and to the right of the colloidal particle. This is so because any surface enclosing the particle should result in the same force; the exact position of S_1 and S_3 in the integration of equation (17) should therefore not matter as long as each of these surfaces remains on its respective side of the particle.

2.3. Results: forces and surface charges

In this article, we seek to obtain an idea as to what effect a dielectric interface will have on the structure of a concentrated colloidal suspension, and this includes, in particular, whether there is an additional wall-induced force acting on an interfacial colloid. In the framework of the interfacial cell theory presented above, we are now in the position to answer this question with the help of equations (14) and (18).

At this point, it is important first to realize that there are two distinct effects relevant in this context. These are: (i) a pure confinement effect and (ii) an image-charge effect. By confinement effect, we mean that the electrolyte is confined to the half-space where $z > 0$ by the very existence of the wall. A spherical double layer around a colloidal particle approaching this wall will therefore become distorted and this distortion will necessarily cost free energy. Therefore, repulsion is to be expected, when the particle is sufficiently close to the wall for this effect to occur.

Image charges exert additional forces on the ions in the interfacial cell. To predict their effect on the colloidal particle, we need to remember that the colloid is located at the centre of a cell that borders not only the dielectric medium (at S_1; see figure 1) but also the next cell (at S_3). The ions inside the interfacial cell will therefore be exposed not only to the image charges from the region $z < 0$ but also to the charges of the neighbouring cell at $z > z_1$. (These charges, of course, do not appear in our computational scheme explicitly, but enter the calculation through the boundary conditions in equation (14).) This is why the actual force in equation (18) is the difference between two terms: one arising from the image charges, $\gamma F(0)$, the other from the charges in the neighbouring cell, $\gamma F(z_1)$.

For all cases where $\eta < 1$, we can thus predict an attractive net force pulling the colloid towards the wall because the image charges with a charge of ηq will exert a force that is—though repulsive—not strong enough to balance the forces from the corresponding ions in the cell at $z > z_1$, i.e. $\gamma F(0) < \gamma F(z_1)$ in equation (18). In the following, we call the effect resulting from this charge imbalance the 'image-charge effect'. Only in the case where $\epsilon' = 0$ ($\eta = 1$) will the image charges be able to match the charges from $z > z_1$, and a totally symmetrical, bulk-like situation is recovered where there is no net force on the colloidal particle, $\gamma F(0) = \gamma F(z_1)$.

Taken together, we have to expect an image-charge-induced attraction and a confinement-induced repulsion of the colloidal particle, and the question now is that of which one dominates and at what particle–wall separation. We could write down the boundary condition at S_3 in equation (14) because we assumed the colloid to be in the centre of its cell, that is at $z_0 = z_1/2$. In this colloidal position, the double layer around the colloid has the same space to extend over

towards S_1 as it has towards S_3. We thus start with the consideration of a situation where there is no confinement effect, but only the image-charge effect. Later we will consider a colloid shifted from the centre position and will allow the two effects to compete with each other.

Figure 2 gives the total force acting on the colloidal particle in the centre of its cell as a function of the ratio ϵ'/ϵ for several values of $Z\tilde{\lambda}_B$ and ϕ_{vol}. The numerical procedure that we have used to solve the PB equation is the same as that in references [32,33]. We first note that, indeed, for a centric position the force acting on the colloid is always attractive and directed towards the wall. We therefore expect the force-free position for the colloid to lie at $z < z_1/2$. Second, our expectations are confirmed in that the imbalance between $\gamma F(0)$ and $\gamma F(z)$ and thus the net force is largest when the image charges vanish, i.e. when $\epsilon' = \epsilon$, and that it is zero when $\epsilon' = 0$. The force increases with growing ϵ'/ϵ, with increasing volume fraction and with increasing colloidal charge, $Z\tilde{\lambda}_B$.

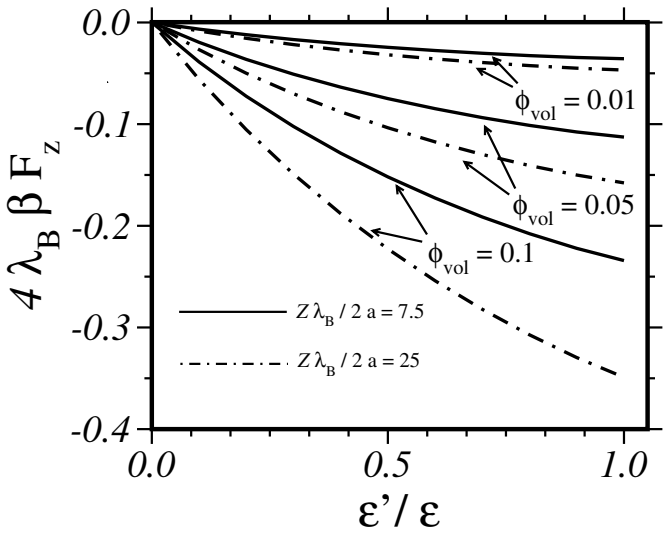

Figure 2. The total force acting on a colloid located at the centre of an interfacial cell for varying ratios of ϵ'/ϵ. The force is attractive and grows with increasing volume fraction ϕ_{vol} and scaled colloidal charge $Z\lambda_B/2a$.

It is also interesting to have a look at the partial forces, $\gamma F(0)$ and $\gamma F(z_1)$, whose difference gives the net force, see equation (18). In figure 3 we show $\gamma F(0)$ as a function of $Z\tilde{\lambda}_B$ for the two limiting cases $\epsilon'/\epsilon = 0$ and $\epsilon'/\epsilon = 1$. Three different volume fractions are considered again. The $\gamma F(z_1)$ plot is not shown because it lies, for both cases $\epsilon'/\epsilon = 0$ and $\epsilon'/\epsilon = 1$, directly on top of the $\gamma F(0)$ curve of the $\epsilon'/\epsilon = 0$ calculation. This is not an unimportant observation because it demonstrates that changes at the one end of the cell, that is at $z = 0$, have no effect on the density and field distribution at the other end, i.e. at $z = z_1$. So the changes in the double layer induced by the dielectric wall take place—for all cases of practical relevance—on a scale much smaller than the mean distance z_1 between the colloidal particles of the suspension.

The difference between the dashed–dotted and the solid line in figure 3 gives the net force at $\epsilon'/\epsilon = 1$ in figure 2. We observe that this net force is much smaller than the partial forces $\gamma F(0)$ and $\gamma F(z_1)$. $\gamma F(0)$ shows furthermore a saturation behaviour which can be traced to the well-known phenomenon of ion condensation, a typical feature of non-linear PB theory [27]. Similar behaviour is found when quantities like the effective charges are plotted [28]. Due to

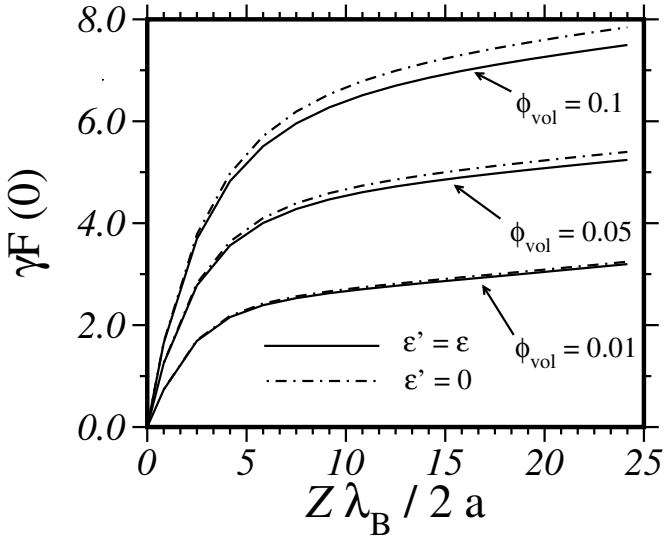

Figure 3. The partial force $\gamma F(0)$ acting on the centred colloid from the wall side as a function of the colloidal charge. The total net force follows if the force $\gamma F(z_1)$ acting from the bulk side is subtracted, equation (18). $\gamma F(z_1)$ lies on top of the $\gamma F(0)$ curve for $\epsilon' = 0$, since this ϵ'-value leads back to a bulk situation where there is no force acting on the colloid and thus $F(0) = F(z_1)$.

this saturation behaviour, the force curves in figure 2 for higher colloidal charges approach a common limiting curve which is not much different from the curve for $Z\tilde{\lambda}_B/2 = 25$. Varying $Z\tilde{\lambda}_B/2$ between 0 and 25, we have thus scanned the most important regime; going any further would not provide more information.

A key to utilizing these curves for experiments lies in the fact that they are of help for estimating the wall-induced forces. Often there are additional surface charges at the interface and the question might arise of whether effects coming from the dielectric discontinuity then become comparatively negligible or not. This can be estimated by comparing the real surface charges with the polarization charges, an aspect of the problem that we study using figure 4. We there show the derivative of the electrostatic potential at $z = 0$, $\partial_z\Phi(0)$ (which is equal to $-e\beta$ times the electric field, $E_z(0)$). This can be identified with a dimensionless polarization surface charge density $4\pi\tilde{\lambda}_B\tilde{\sigma}_{pol}$. In the BVPs of equations (7) and (14), these polarization charges are identical to the first term in the r.h.s. of the boundary condition for the S_1-boundary. The second term, $4\pi\tilde{\lambda}_B\tilde{\sigma}$, accounts for any additional interfacial charges that one would have to add to these polarization charges. With respect to a specific experiment, one has to compare these two terms with the help of the data of figure 4 in order to be able to determine the relative importance of polarization charges. The curves for smaller volume fractions and ϵ' look similar, but the polarization charges are always smaller. Note that, as a result of the ion condensation, the curves again approach a limiting curve with increasing colloidal charge. So, for a rough estimate of image-charge effects in colloidal systems with charges higher than $Z\tilde{\lambda}_B/2 = 25$, one can use this limiting curve.

Next, we want to displace the colloid from its centre position to see how important the confinement effect is relative to the image-charge effect considered so far. The problem with a colloidal position $z_0 \neq z_1/2$ is that the plane of symmetry between the shifted colloid in the interfacial cell and the centric colloid at $z = 3z_1/2$ in the next-neighbour cell is no longer at $z_{sym} = z_1$, but is now at $z_{sym} = z_0 + l/2$ where $l = 3z_1/2 - z_0$ is the relative separation

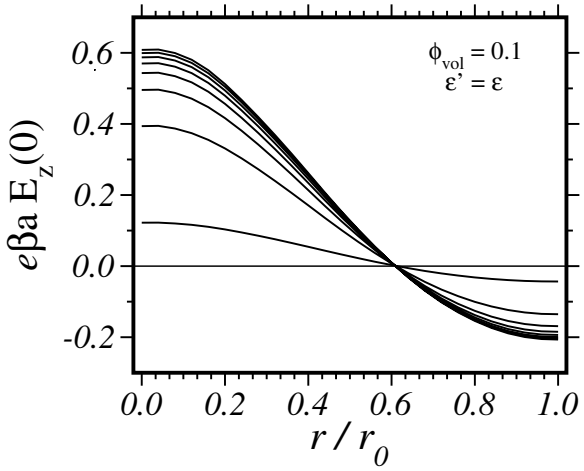

Figure 4. The normal component of the electric field at the dielectric interface as a function of the radius r. This electric field is equivalent to the surface polarization charge density induced by the dielectric discontinuity. The eight curves are for several colloidal charges ($3Z\lambda_B/a = 5, 25, 45, 65, 85, 105, 125, 145$ from bottom to top).

of the colloids. For $z_0 < z_1/2$, z_{sym} is inside the interfacial cell. Thus, the plane where the normal electric field vanishes is not at S_3 any more, contrary to what we have assumed for the boundary S_3 in the BVP of equation (14). The question thus is that of what boundary condition to use at S_3 in equation (14). This question is answered in the appendix, where we explain how one can generate these boundary conditions from another BVP.

Figure 5 now shows the partial forces $\gamma F(0)$ and $\gamma F(z_1)$ in equation (18) for two different positions of the colloid, namely $z_0 = z_1/2$ and $z_0 = 2z_1/5$. The curves for the centric position are the same as in figure 3. They show the image-charge effect where, due to the disappearance of the image charges ($\epsilon' = \epsilon$), the imbalance between the image charge distribution at $z < 0$ and the charge distribution at $z > z_1$ is most pronounced, so $\gamma F(0)$ is invariably smaller than $\gamma F(z_1)$. The resultant force is attractive. For $z_0 = 2z_1/5$ however this changes: $\gamma F(0)$ now becomes much larger than $\gamma F(z_1)$ due to the confinement effect and the net force on the colloid becomes highly repulsive for all colloidal charges. For $z_0 = 0.4z_1$, we also added the force curve $\gamma F(0)$ for the case $\epsilon' = 0$ where there is no image-charge effect. This comparison shows that when allowing for the image-charge effect, an attractive force becomes observable which, however, is not strong enough to overcome the confinement-induced repulsion. Thus, at $z_0 = 0.4z_1$ we have already reached a wall–particle distance where the confinement effect dominates over the image-charge effect. The minimum (force-free) position of the colloid will therefore lie somewhere between $0.4z_1$ and $0.5z_1$. In fact, its exact position is roughly at $0.45z_1$ for all scaled colloidal charges and all volume fractions considered (0.001 to 0.3). Note, however, that z_1 itself depends on the volume fraction so the absolute minimum positions vary considerably with the volume fraction.

3. Monte Carlo simulation

As a major result of this work we have seen that for wall–particle distances smaller than approximately $z_1/2$, i.e. smaller than half of the mean bulk colloid–colloid distance, the forces on the colloid become invariably repulsive due to the strong-confinement effect, irrespective of

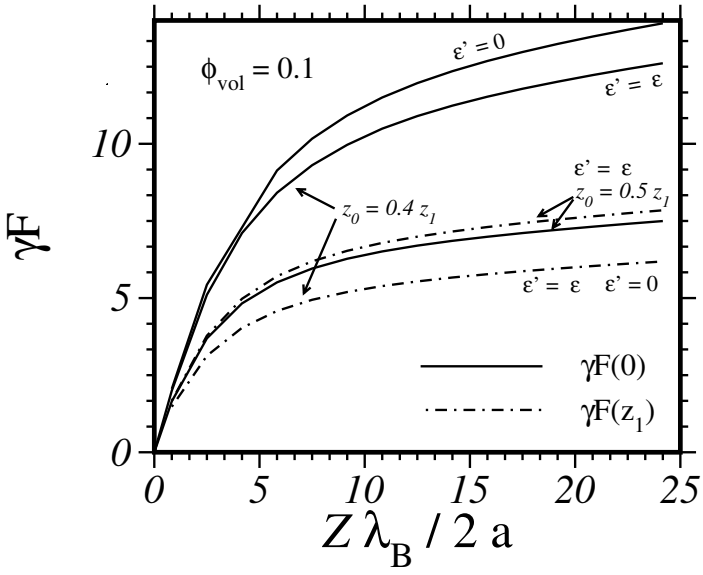

Figure 5. Partial forces $\gamma F(0)$ and $\gamma F(z_1)$ for two different positions $z_0 = 0.4z_1$ and $z_0 = 0.5z_1$ of the colloid in the interfacial cell. While in the centre position $\gamma F(0)$ is always smaller than $\gamma F(z_1)$, it becomes greater than $\gamma F(z_1)$ when the colloid is slightly shifted towards the wall. Accordingly, the total force acting on the colloid becomes repulsive.

the presence of image charges. In this section, we look into the question of whether this result is changed when the counterions are allowed to have a finite core radius. Since this cannot be treated within the PB scheme presented above, we have performed MC simulations. To see how big the finite-size effect can become, we study the extreme situation where a colloid is touching the dielectric wall. Here finite-size effects can be expected to be most pronounced because of the spatial confinement of the ions in the narrow region between the colloid and the wall. For counterions with both finite and zero radius, we will calculate the free energy of a colloid in such a touching position and compare it with the free energy of a colloid in a bulk situation. If this energy difference is positive and only weakly dependent on the counterion radius, we may conclude that the results of the previous section remain the same even for counterions of finite size.

3.1. Computational details

Our MC simulation set-up is based on a cubic cell model—a macroion of radius a and charge Ze in a cubic cell of length L ($x \in [-L/2, L/2]$, $y \in [-L/2, L/2]$, and $z \in [0, L]$) neutralized by inhomogeneously distributed microions and suspended in water of dielectric constant $\epsilon = 78.3$. The cell model MC simulation is usually performed in a fixed configuration of the single macroions while the microions explore the configuration space. In the bulk situation, it is conventional to fix the macroion at the body centre of the cubic cell. Hence the macroion is located at the Cartesian position $(x, y, z) = (0, 0, L/2)$. We shall call this the bulk scheme (BS). Here, no dielectric interface is involved and hence no surface polarization effects. In the second scheme, the dielectric interface scheme (DS), the macroion is made to touch the ϵ'-dielectric wall at $z = 0$, i.e., its position is at $(0, 0, a)$.

The simulations were performed in the canonical ensemble at room temperature

corresponding to a Bjerrum length $\lambda_B = e^2/(\epsilon k_B T) = 7.14$ Å. The cell volume (and thus L) is determined by the macroion volume fraction $\phi_{vol} = V_m/L^3$. In the following simulations, $\phi_{vol} = 0.01, 0.05, 0.10$ are investigated. We again consider the salt-free case where the microions are all monovalent counterions. We have already noticed that the PB equation then scales with $Z\lambda_B/a$. Beyond the mean-field level, this, of course, ceases to be valid, and our MC results will also depend on the ratio λ_B/a. We study values for $\lambda_B/2a$ ranging from $\lambda_B/2a = 0.6$ (small particle) to $\lambda_B/2a = 0.03$ (large particle).

In each scheme, the macroion remains fixed, and the counterions are moved through the cell to sample the configuration space according to the traditional Metropolis algorithm [36]. Periodic boundary conditions, the minimum image convention, and Ewald summation schemes [37,38] are not applied in summing the Coulomb interactions. This is a consequence of the cell model which assumes that contributions from neighbouring cells are negligible. The validity of this approximation has been tested against a periodically repeated system where the Ewald summation scheme was applied [29, 31]. In the DS, the situation is similar to that of an electrolyte confined between a charged and an uncharged planar wall, described by Wennerström *et al* [22].

In the BS, the total configurational potential energy of the ions:

$$U = \sum_{i<j} u_{ij}(r_{ij}) \tag{20}$$

is averaged over the simulation, calculated in each run using the pair interaction potential

$$\beta u_{ij}(r_{ij}) = u_{ij}^{rep} + \frac{q_i q_j \lambda_B}{r_{ij}} \tag{21}$$

where the charge valence q_i is Z ($5 \leqslant Z \leqslant 300$) for the macroion and -1 for the counterions. The term u_{ij}^{rep} is a repulsive hard-sphere interaction:

$$u_{ij}^{rep} = \begin{cases} \infty & \text{if } r_{ij} < d_{ij} \\ 0 & \text{if } r_{ij} > d_{ij} \end{cases} \tag{22}$$

where d_{ij} is the minimum distance of the centres of the ith and jth ions. $d_{ij} = (d_m + d_c)/2$ for macroion–counterion interaction, and $d_{ij} = d_c$ for counterion–counterion interaction, with $d_m = 2a$ being the macroion diameter. The counterion diameter d_c was chosen to be zero (point ion) and 4.25 Å.

In the DS scheme, the electrostatic image charges of all ions in the solvent have to be taken into account. An ion i with charge $q_i e$ and coordinate (x_i, y_i, z_i) in the positive half-space, $z > 0$, has an image i' located at $(x_i, y_i, -z_i)$ in the ϵ'-medium whose charge is $q_i' e = \eta q_i e$ with η defined in equation (8). These image charges contribute to the potential in the ϵ-medium; hence the total internal energy U, for N real ions in the cell, becomes the sum of contributions from the real charges, equation (21), and image charges (u^{im}). Thus,

$$U = \sum_{i<j} \left[u_{ij}(r_{ij}) + u_{ij}^{im}(r_{ij}) \right] + \sum_i u_i^{im}(z_i) \tag{23}$$

where $u_{ij}(r_{ij})$ is the real-charge contribution, equation (21),

$$\beta u_{ij}^{im}(r_{ij}) = \lambda_B \frac{\eta q_i q_j}{[x_{ij}^2 + y_{ij}^2 + (z_i + z_j)^2]^{1/2}} \tag{24}$$

is the real–image-charge pair interaction potential, and

$$\beta u_i^{im}(z_i) = \lambda_B \frac{\eta q_i^2}{4 z_i} \tag{25}$$

is the interaction potential of a real charge with its own image charge (self-image potential energy). The factor $\frac{1}{2}$ that appears explicitly in the self-image energy and implicitly in the $u_{ij}^{im}(r_{ij})$ pair energies is clarified in the appendix.

The total configurational energies were averaged over the simulation as in the previous scheme. For both schemes, in each MC run, the system was equilibrated for about 45 000–90 000 MC cycles, depending on the Coulomb coupling strength, and averages taken in the next 15 000–30 000 cycles. One MC cycle here corresponds to an attempted move of all mobile ions in the system. Equilibration was ensured by arriving at roughly the same energy by starting the simulation from a completely random configuration corresponding to infinite temperature, and starting from a condensed configuration of the counterions on the macroions.

3.2. Monte Carlo simulations: results and discussion

The scaling of the PB equation with $Z\lambda_B/2a$ has been demonstrated by Groot [29] for the effective macroion charges. Likewise, the configurational energy per counterion scales with $Z\lambda_B/2a$ in the sense that $\beta\langle U\rangle/Z = f(Z\lambda_B/2a)$, where f is a unique function and $\langle U\rangle$ is the averaged energy. This scaling behaviour implies that properties of particles, whose simulation is currently impossible (for instance, micron particles with $Z \sim 10^4$), can be extrapolated from data for particles that can easily be simulated. For example, if we characterize a system whose coupling strength is $Z\lambda_B/2a = 10$ (i.e. $\lambda_B/2a = 0.1$, $Z = 100.0$), then we can predict the behaviour of all systems with the same coupling strength (e.g. $\lambda_B/2a = 0.01$, $Z = 1000.0$).

Figure 6 shows the energy per ion $\beta\langle U\rangle/Z$ against the scaled macroion charge $\lambda_B Z/2a$, in the bulk situation, together with the PB scaling function. Consistently with Groot's observation for effective charges [29], the MC energies gradually move away from perfect scaling shown by the PB function (which provides the upper limit), as the coupling increases from $\lambda_B/2a = 0.03$ (large particle, $d_m = 238$ Å in water) to $\lambda_B/2a = 0.6$ (small particle, $d_m = 11.9$ Å). This behaviour is due to ion–ion correlation among the counterions which is well accounted for in MC simulation but neglected by PB theory. Figure 6 confirms once more the well-known fact that PB theory becomes correct in the limit $\lambda_B/a \to 0$.

A more interesting result is the quantity $\beta\Delta\langle U\rangle/Z = \beta(\langle U_{DS}\rangle - \langle U_{BS}\rangle)/Z$ which measures the electrostatic internal energy gain or loss per counterion between the two schemes (BS and DS), as a function of $Z\lambda_B/2a$. $\beta\Delta\langle U\rangle/Z$ versus $Z\lambda_B/2a$ is shown in table 1 for two different counterion radii and a size ratio $\lambda_B/2a = 0.03$ which in figure 6 we have seen to lie nearest to the PB solution. In the following, we will leave this parameter unchanged. Furthermore, we consider a ratio of dielectric constants, $\epsilon'/\epsilon = 0.08$, typical of a glass–water interface ($\epsilon = 78.3$, $\epsilon' = 6.3$, $\eta = 0.85$).

The result shows *negative* $\beta\Delta\langle U\rangle/Z$ values for high $Z\lambda_B/2a$ coupling for all values of ϕ_{vol} and d_c considered. This means that from the purely electrostatic point of view, the situation where the colloid touches the wall can become energetically more favourable than the bulk situation where it is in the centre of its cell in an isotropic environment, a result that at first looks surprising considering the large repulsive self-image interaction, equation (25), of the colloid in the DS. This crossover behaviour of $\beta\Delta\langle U\rangle/Z$ with increasing coupling strength can be understood as follows: the positive $\beta\Delta\langle U\rangle/Z$ for small $Z\lambda_B/2a$ is in the regime of small electrostatic coupling, where the density profile is only weakly sensitive to both the position of the colloidal particle and the image charges. The positive value of $\beta\Delta\langle U\rangle/Z$ is then caused by the strong (unscreened) repulsion of the colloid by its own image. The change of sign of this quantity in the regime of strong electrostatic coupling, on the other hand, can be attributed to the fact that there are many more counterions attracted to the colloidal surface in the DS than in the BS. This is due to the immediate neighbourhood of the colloid (with charge Z) and

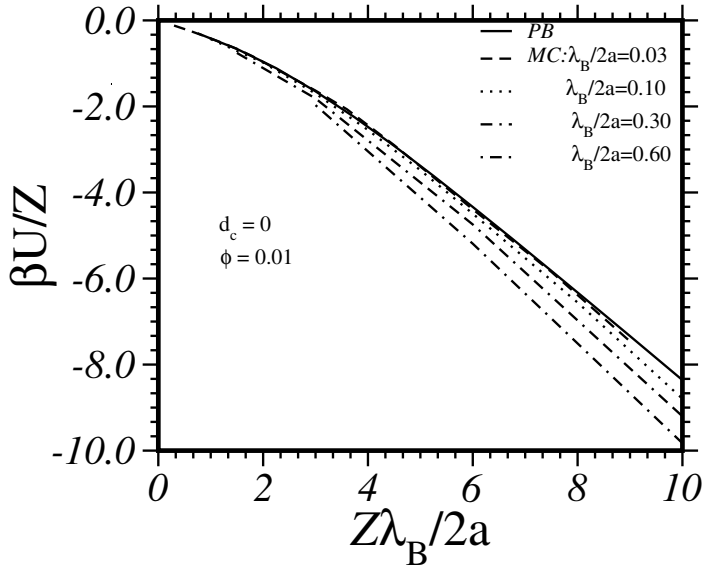

Figure 6. The average total internal energy per counterion, $\beta\langle U\rangle/Z$, as a function of the scaled colloidal charge, $Z\lambda_B/2a$. The solid line is the result from the PB cell theory, while the other lines are results of MC simulations for the various values of the scaling parameter $\lambda_B/2a$. All points in the figure were obtained at 1% macroion volume fraction with point counterions ($d_c = 0$).

Table 1. The variation of $\beta\Delta\langle U\rangle/Z$ with the macroion charge Z for $\lambda_B/2a = 0.03$ coupling, and various simulation parameters. $\Delta\langle U\rangle$ is the average electrostatic energy difference between the bulk and dielectric wall MC schemes. ϕ_{vol} is the macroion volume fraction and d_c is the diameter of the counterions. The negative values of $\Delta\langle U\rangle$ show where adsorption of the macroion at the dielectric wall (DS scheme) is energetically favoured.

	$\beta\Delta\langle U\rangle/Z$					
	$\varepsilon' = 0.08\varepsilon$					$\varepsilon' = \varepsilon$
	$d_c = 0$		$d_c = 4.25$ Å			$d_c = 4.25$ Å
$Z\lambda_B/2a$	$\phi_{vol} = 0.01$	$\phi_{vol} = 0.10$	$\phi_{vol} = 0.01$	$\phi_{vol} = 0.05$	$\phi_{vol} = 0.10$	$\phi_{vol} = 0.01$
0.3	0.08749		0.08513	0.06045	0.05053	0.02220
0.6	0.15287	0.07664	0.15245	0.09893	0.07797	0.04369
0.9	0.20458	0.09419	0.20360	0.12171	0.09417	0.05661
1.2	0.23075	0.10485	0.23258	0.14201	0.10505	0.06748
1.5		0.10945	0.24198		0.11160	0.07580
1.8	0.23519	0.09452		0.13425	0.11693	0.08318
2.4	0.18507		0.19806	0.09407		0.07630
3.0	0.09337	0.07020	0.16141	0.08846	0.10143	0.09544
3.6	−0.01140	0.05329	0.09707		0.07570	0.02965
4.5	−0.10738			0.04461	0.05500	
6.0	−0.12685	−0.00540	−0.08560		0.00491	−0.01648
7.5		−0.02259	−0.17947	−0.04457	−0.02501	−0.03931
9.0	−0.13259	−0.02582	−0.19853	−0.06526	−0.03933	−0.05583

its image (with charge ηZ) in the wall situation where the counterions are now attracted by a total charge $(1 + \eta)Z = 1.85Z$ which is much larger than the colloidal charge Z in the BS. The preferred region for these counterions is the wedge region between the colloid surface and

the wall where the counterion density is particularly high. This high density, together with the spatial confinement, explains why finite-size effects of the microions become non-negligible, as comparison of the values for $d_c = 0$ and $d_c = 4.25$ at $Z\lambda_B/2a = 9.0$ and $\phi_{vol} = 0.1$ in table 1 reveals.

We have not yet taken account of the entropic effect due the inhomogeneous distribution of the counterions in the system. Actual adsorption should be determined from the total free energy. A direct determination of free energy or entropy is not possible from the present MC simulations [37,38]. Nevertheless, we can determine the total free-energy difference ΔA from $\Delta\langle U\rangle$ calculated above through the following integration [39]:

$$\frac{\beta\Delta A}{Z} = \int_0^\beta \frac{\Delta\langle U\rangle}{Z}\,\mathrm{d}\beta' \tag{26}$$

which by a change of variables we transform into an integral over the function $f(x) := \beta\Delta\langle U(x)\rangle/Z$ with $x = Z\lambda_B/2a$:

$$\frac{\beta}{Z}\Delta A(Z\lambda_B/2a) = \int_0^{Z\lambda_B/2a} f(x)\,\mathrm{d}x. \tag{27}$$

The free-energy difference as a function of $Z\lambda_B/2a$ is plotted in figure 7 for the two cases $\epsilon'/\epsilon = 0.08$ and $\epsilon'/\epsilon = 1$, i.e., when the image charges are fully switched on ($\eta \approx 1$ if $\epsilon'/\epsilon = 0.08$) and non-existent ($\eta = 0$ if $\epsilon'/\epsilon = 1$). Figure 7 reveals that (i) the free-energy barrier between a centric bulk and a wall position of the colloid is always positive, for all cases considered, (ii) the effect of the finite size of the counterions is relatively small, and finally, (iii) with increasing volume fraction and when switching off the image charges ($\epsilon' = \epsilon$), the height of the barrier is reduced.

We have seen from table 1 that the configurational energy difference for large coupling strength becomes negative. The positive free-energy difference of figure 7 must therefore

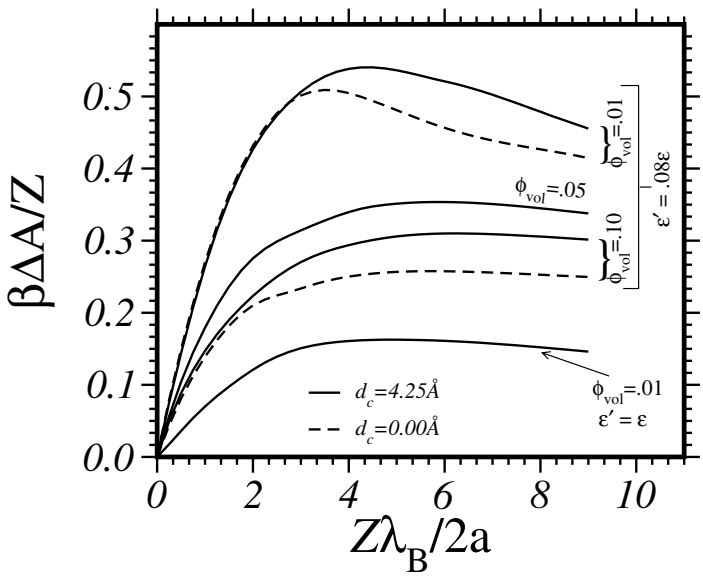

Figure 7. The average free-energy difference per counterion, $\beta\Delta A/Z$, obtained by integrating the $\beta\Delta\langle U\rangle/Z$ of table 1. The labels are as defined in table 1. The plots show that adsorption of a macroion on the dielectric wall is not favoured in all aspects investigated. There are no negative $\beta\Delta A/Z$.

be due to a negative entropy difference that overcompensates $\beta\Delta\langle U\rangle/Z$. In view of the confinement effect analysed in the previous section, the explanation for this can obviously be found in the reduction of counterion entropy due to the distortion of the double layer from its spherical shape when the colloid touches the wall. We thus again end up by recognizing that for small wall–particle distances this confinement effect is the dominating mechanism that prevents the colloid from becoming adsorbed onto the wall. Figure 7 indicates that this result remains unchanged even if the counterions have finite size. However, in the limit where the electrostatic internal energy is dominant (vanishing configurational entropy), there exist conditions where the colloid is attracted to its own image ion (having nearly same charge), therefore favouring adsorption.

4. Conclusions and summary

Any charged object in the neighbourhood of an interface between media of different dielectric constants experiences image-charge forces arising from the dielectric discontinuity. In a concentrated suspension of macroions (these can be everything from globular proteins to simple latex particles), these forces compete with the usual double-layer forces between the macroions. A macroion next to such an interface experiences an anisotropic environment: towards the bulk side it has the next-neighbour colloid screened in the usual way by its microions, while towards the wall it sees the image charge of its own charge and those of its double layer. Since the image charges in most experimentally relevant cases are weaker than the real charges, this imbalance leads to an attractive wall-induced force on the colloid.

In this paper, we have been concerned with the question of how strong this attraction can become and whether it could overcome, in principle, the confinement-induced repulsion that is due to the distortion of the double layer through the wall. To answer this question, we have suggested a cell model where the colloid plus its counterions is confined to a finite volume that is just the reciprocal of the colloidal density. The ion distribution inside this cell can then be calculated from the PB equation. Of crucial importance are the boundary conditions at the cell boundaries, because it is through them that the physics of the problem comes into play. By requiring the electric field to vanish at one side of the cell, while accounting for the dielectric jump at the other, we take account of the anisotropic environment of the interfacial colloid, with there being a colloid in the next-neighbour cell, on one side, and an interface, on the other.

The PB equation in the cell can be solved directly only in the special case where $\epsilon' = 0$. If $\epsilon' \neq 0$, then the condition at the interface constitutes a matching condition for the potential on both sides of the interface. We suggested an iterative procedure by means of which these two solutions can be linked together. That the PB equation scales with $Z\lambda_B/a$ in the salt-free limit has proven to be of great help in reducing the number of independent variables of the problem. Concentrating on image-charge effects (no interfacial charges), we are left with three parameters governing the problem, namely: ϵ'/ϵ, $Z\lambda_B/a$, and the volume fraction ϕ_{vol}. Working through all three parameters in a systematic way, we have obtained the following results:

(i) For wall–particle distances z_0 a little smaller ($z_0 \approx 0.4z_1$) than half of the mean bulk colloid–colloid distance z_1, the forces on the colloid become invariably repulsive due to the strong-confinement effect. This holds for all values of ϵ'/ϵ between zero and one, all volume fractions, and all scaled colloidal charges $Z\lambda_B/a$. That the latter statement is true even though we could only go up to values of $Z\lambda_B/2a = 25$ follows from the fact that because of ion condensation the forces on the colloid show a saturation behaviour for growing colloidal charge. Values for scaled charges higher than $Z\lambda_B/2a = 25$ will

therefore not produce new results.

(ii) As a result of this dominating confinement effect, we can therefore conclude that for a broad class of suspensions, a major structural rearrangement of the colloidal suspension near a dielectric interface is not to be expected. This should remain true even if allowance is made for dispersion forces which are much shorter ranged than double-layer forces.

(iii) The relative importance of interfacial surface charges for the interfacial structure problem of suspensions of spherical macroions can be estimated from our results by comparing them with the polarization surface charge density calculated in figure 4. Only if the density of the interfacial charges is much larger than the density of the polarization charges may a significant effect on the colloids be expected.

(iv) In our MC simulation, we have proposed a cell model in the cubic approximation of the Wigner–Seitz cell where the macroion is fixed on the surface of the dielectric interface which results in: (a) distortion of the counterionic atmosphere around the colloid and (b) the maximum effect of the surface polarization due to image charges. Free-energy calculation for the class of dielectric interfaces investigated ($\varepsilon' \ll \varepsilon$) reveals that this adsorbed configuration of the macroion is never favoured relative to the bulk situation where confinement and image-charge effects are negligible. This result holds for both finite-size and point-like counterions.

Acknowledgments

We thank Rudolf Klein and Roland Netz for many helpful discussions. Financial support from the Deutsche Forschungsgemeinschaft (SFB 513) is gratefully acknowledged.

Appendix

A.1. The image-charge concept and the Poisson–Boltzmann equation

Let us begin by recalling the basic idea of the image-charge concept for a purely electrostatic problem [40]. As in section 2, we use cylindrical coordinates. Let $V = f(r, z)$ be the potential for all z, if the whole space has a dielectric constant ϵ and all charges are confined to $z > 0$. Replacing now the dielectric medium in $z < 0$ by another material with a dielectric constant ϵ', one can obtain the new potential from the old one through

$$V = \begin{cases} f(r, z) + \eta f(r, -z) & z \geqslant 0 \\ (1 + \eta) f(r, z) & z < 0 \end{cases} \tag{A.1}$$

with η from equation (8). This new potential is continuous across the interface and its derivative at $z = 0$ satisfies the matching condition

$$\epsilon \, \partial_z V\big|_{z=0+} = \epsilon' \, \partial_z V\big|_{z=0-}. \tag{A.2}$$

The advantage of this scheme is that we can use the solution to the unbounded problem for the interfacial problem.

This idea cannot naively be applied to a PB problem where mobile charges are involved. This is so because the PB equation is a differential equation depending in a non-linear way on the potential. If $f(r, z)$ solves the PB equation in the unbounded problem, a construction like that in equation (A.1) does *not* give a solution to the PB equation in the bounded problem, as we will show now.

We look for a potential V that satisfies the Laplace equation

$$\nabla^2 V = 0 \qquad S' \colon \partial_n V = 0 \tag{A.3}$$

for $z < 0$ and the PB equation

$$\nabla^2 V = \kappa^2 \mathrm{e}^V \qquad S\colon \partial_n V = 0 \tag{A.4}$$

for $z > 0$. At the interface S_1 ($z = 0$), the two equations are linked together through the matching condition, equation (A.2), and the requirement that V must be continuous at $z = 0$. The surface S defines the boundary (excluding S_1) of the region where we want to solve the PB equation. S' is the mirror image ($z \to -z$) of this surface. At this boundary we fix the derivative of the potential, $\partial_n V$, in a direction normal to the surface.

Substituting now the potential, equation (A.1), into equations (A.3) and (A.4), we find

$$\nabla^2 f = 0 \qquad S'\colon \partial_n f = 0 \tag{A.5}$$

for $z < 0$ and

$$\nabla^2 f(r, z) = \kappa^2 \mathrm{e}^{f(r,z)} \mathrm{e}^{\eta f(r,-z)} \qquad S\colon \partial_n f = 0 \tag{A.6}$$

for $z > 0$, where in the last equation we have used equation (A.5). The matching conditions at S_1 become

$$\partial_z f\big|_{z=0+} = \partial_z f\big|_{z=0-} \tag{A.7}$$

and

$$f\big|_{z=0+} = f\big|_{z=0-} \tag{A.8}$$

which is nothing but the requirement that f must be continuously differentiable over the whole space (in particular at $z = 0$, equations (A.7) and (A.8)). This reduction to one continuously differentiable function is very much like that in the purely electrostatic case. However, in contrast to the electrostatic case, we still have the variable η appearing in equation (A.6). It enters through the non-linearity of the PB equation. The function f at $z > 0$ depends on the function f at $z < 0$, and it is therefore not possible to reduce the problem to determining a function for the unbounded system, as in the electrostatic problem. The problem can again be solved iteratively, only.

A.2. Boundary conditions for eccentric colloidal positions

We here want to explain briefly how one can find the correct electric field distribution for the boundary condition at S_3 in the BVP of equation (14), if the colloid is *not* in the centre of its cell but at a position $z_0 < z_1/2$. The colloid in the next-neighbour cell is assumed to remain in its centre position which is at $z = 3z_1/2$. Thus, the separation of the two colloids is $l = 3z_1/2 - z_0$ and the plane of symmetry is at $z_{sym} = z_0 + l/2$, which is a distance $l_{sym} = z_1 - z_{sym} = z_1/4 - z_0/2 > 0$ away from S_3 inside the interfacial cell, $z_{sym} < z_1$. What then is the electric field distribution at z_1 and thus the boundary condition at S_3?

We want to answer this question with the help of a little extra calculation. Let us consider two different problems. In problem (a) the interfacial colloid is located a z_0 and the colloid in the next-neighbour cell at $3z_1/2$. This is our original problem. In problem (b) the interfacial colloid is situated at $z_{00} = z_1/4 + z_0/2$ (with z_0 taken from problem (a)), while the colloid in the neighbour cell is positioned at $z_{00} + l$ with $l = 3z_1/2 - z_0$. This is our reference problem, where both colloids are shifted the same distance away from their respective centre positions, but in opposite directions. In the two problems the colloid–colloid distance is the same, but the absolute positions of the plane of symmetry are different: it is at $z_1 - l_{sym}$ in problem (a) and actually at z_1 in problem (b). Thus, problem (b) leads again to a BVP like that in equation (14) where the boundary conditions at S_3 are known.

If we now assume that field and density distributions *between* (and only between) the two colloids are the same in the two problems, we are allowed to take the solution of problem (b) to

generate the appropriate boundary condition for problem (a). That this assumption is justified follows from our observation made earlier that the density and field distributions at S_3 are not at all affected by any change in the boundary conditions at S_1. This is also why the choice of the boundary condition at S_1 in equation (14) for our reference problem (b) is unimportant. The boundary condition for $\epsilon' = 0$ is certainly the most convenient choice.

From the solution of the reference problem, we can determine the electric field distribution at $z = z_1 + l_{sym}$ which is just the negative of the distribution at $z = z_1 - l_{sym}$. The radial distribution of the z-component of the electric field, $-e\beta E_z(r)$, at this point is what we are now looking for: the desired field distribution for the boundary S_3 in problem (a). The corresponding BVP is identical to equation (14), except for the last line which we now have to replace by

$$S_3: \qquad \partial_z \Phi^{(n)} = -e\beta E_z(r). \tag{A.9}$$

Note that this procedure for finding a boundary condition from another BVP is justifiable only if one can be sure that changes of the boundary condition at S_1 have no effect on the field and density distributions at S_3.

A.3. The electrostatic potential energy across planar dielectric interfaces

Let us consider, for simplicity, only two ions i and j (each having a single charge e) located respectively at $\vec{r}_i = (x_i, y_i, z_i)$ and $\vec{r}_j = (x_j, y_j, z_j)$ in a medium of dielectric constant ε, and close to a wall of dielectric constant ε'. This results in the formation of image charges i' and j' located at $\vec{r}_{i'} = (x_i, y_i, -z_i)$ and $\vec{r}_{j'} = (x_j, y_j, -z_j)$ respectively for i and j. Then the relative distances between the ions (real and image) are: r_{ij} for i and j, $r_{ij'}$ for i and j', $r_{i'j}$ for j and i', $r_{ii'} = 2z_i$ between i and i', and finally $r_{jj'} = 2z_j$ between j and j'. The potential ψ at the position of i is

$$\psi_i = \frac{e}{\varepsilon r_{ij}} + \frac{\eta e}{\varepsilon r_{ij'}} + \frac{\eta e}{2\varepsilon z_i} \tag{A.10}$$

where $\eta e = e(\varepsilon - \varepsilon')/(\varepsilon + \varepsilon')$ is the charge on an image ion. The first term is due to the real ion j, the second due to its image j', and the third term is from the self-image i'. The potential at j is the same as equation (A.10) except that i and j are interchanged. Therefore the total electrostatic potential energy:

$$\beta U = \frac{\beta}{2} \int \rho\psi \, \mathrm{d}V$$

for a system of ions now becomes

$$\beta U = \frac{\lambda_B}{r_{ij}} + \frac{\lambda_B \eta}{2}\left(\frac{1}{r_{ij'}} + \frac{1}{r_{i'j}} + \frac{1}{2z_i} + \frac{1}{2z_j}\right). \tag{A.11}$$

This equation cleanly separates into purely real (first term) and real–image-charge interactions, showing explicitly the factor $1/2$ in the real–image interaction. For planar interfaces, $r_{ij'} = r_{i'j}$. We can generalize equation (A.11) for N ions each of charge $q_k e$ in the region ε, and find

$$\beta U = \lambda_B \sum_{i<j}^{N}\left(\frac{q_i q_j}{r_{ij}} + \frac{\eta q_i q_j}{r_{ij'}}\right) + \frac{\lambda_B}{2}\sum_{i=1}^{N}\frac{\eta q_i^2}{2z_i}. \tag{A.12}$$

In (A.12) the factor $1/2$ is implicit in the real–image pair interaction and care must be taken to avoid double counting.

References

[1] Schmitz K S 1993 *Macroions in Solution and Colloidal Suspension* (New York: VCH)
Evans D F and Wennerström H 1994 *The Colloidal Domain: Where Physics, Chemistry, Biology, and Technology Meet* (New York: VCH)
Nägele G 1996 *Phys. Rep.* **272** 215

[2] Allahyarov E, D'Amico I and Löwen H 1998 *Phys. Rev. Lett.* **81** 1334
Goulding D and Hansen J-P 1999 *Europhys. Lett.* **46** 407
Bowen W R and Sharif A O 1998 *Nature* **393** 663
Neu J C 1999 *Phys. Rev. Lett.* **82** 1072
Allahyarov E, D'Amico I and Löwen H 1999 *Phys. Rev.* E **60** 3199

[3] Goulding D and Hansen J-P 1998 *Mol. Phys.* **95** 649

[4] Earnshaw J C 1986 *J. Phys. D: Appl. Phys.* **19** 1863
Haughey D and Earnshaw J C 1996 *Colloids Surf.* A **106** 237
Hurd A J 1985 *J. Phys. A: Math. Gen.* **18** 1055

[5] Tandon S, Kesavamoorthy R and Asher S A 1998 *J. Chem. Phys.* **109** 6490
Kesavamoorthy R, Rajalakshmi M and Balu Rao C 1989 *J. Phys.: Condens. Matter* **1** 7149
Kesavamoorthy R, Balu Rao C and Tata B V R 1991 *J. Phys.: Condens. Matter* **3** 7973

[6] Firshein W 1989 *Annu. Rev. Microbiol.* **43** 89
Verma I M and Somia N 1997 *Nature* **389** 239
Behr J P 1994 *Bioconjugate Chem.* **5** 382
Maier B and Rädler J O 1999 *Phys. Rev. Lett.* **82** 1911
Rädler J O, Koltover I, Salditt T and Safinya C R 1997 *Science* **275** 810

[7] Gambu I and Roux B 1997 *J. Phys. Chem.* B **101** 6066

[8] Forsten K E, Kozack R E, Lauffenburger D A and Subramanian S 1994 *J. Phys. Chem.* **98** 5580

[9] Kepler G M and Fraden S 1994 *Phys. Rev. Lett.* **73** 356
Crocker J C and Grier D G 1996 *Phys. Rev. Lett.* **77** 1897
Grier D G 1998 *Nature* **393** 621

[10] Ghezzi F and Earnshaw J C 1997 *J. Phys.: Condens. Matter* **9** L515
Larsen A E and Grier D G 1997 *Nature* **385** 230

[11] Hurd A J and Schaefer D J 1985 *Phys. Rev. Lett.* **54** 1043

[12] Pieranski P 1980 *Phys. Rev. Lett.* **45** 569

[13] Pieranski P 1985 *Phys. Rev. Lett.* **55** 226

[14] Van Blaaderen A and Wiltzius P 1995 *Science* **270** 1177
Grier D G and Murray C A 1991 *J. Chem. Phys.* **100** 9088

[15] Fisher M E, Levin Y and Li X 1994 *J. Chem. Phys.* **101** 2273

[16] Torrie G M, Valleau J P and Patey G N 1982 *J. Chem. Phys.* **76** 4615

[17] Bratko D, Jönsson B and Wennerström H 1986 *Chem. Phys. Lett.* **128** 449

[18] Kjellander R and Marcelja S 1984 *Chem. Phys. Lett.* **112** 49

[19] Levine S and Outhwaite C W 1978 *J. Chem. Soc. Faraday Trans.* II **74** 1670

[20] Linse P 1986 *J. Chem. Phys.* **90** 6821

[21] Hill T L 1960 *Statistical Mechanics* (Reading, MA: Addison-Wesley)

[22] Wennerström H, Jönsson B and Linse P 1986 *J. Chem. Phys.* **76** 4665

[23] Stillinger F H 1961 *J. Chem. Phys.* **35** 1584

[24] Schmutzer E 1955 *Z. Phys. Chem.* **204** 131

[25] Netz R R 1999 *Phys. Rev.* E **60** 3174

[26] Barrat J L and Joanny J F 1996 *Adv. Chem. Phys.* **94**

[27] Belloni L 1998 *Colloids Surf.* A **140** 227
Manning G S 1951 *J. Chem. Phys.* **51** 924

[28] Alexander S, Chaikin P M, Grant P, Morales G J, Pincus P and Hone D 1984 *J. Chem. Phys.* **80** 5776

[29] Groot R D 1991 *J. Chem. Phys.* **95** 9191

[30] Gisler T, Schulz S F, Borkovec M, Sticher H, Schurtenberger P, D'Aguanno B and Klein R 1994 *J. Chem. Phys.* **101** 9924

[31] Stevens M J, Falk M L and Robbins M O 1996 *J. Chem. Phys.* **104** 5209

[32] von Grünberg H H and Belloni L 2000 *Phys. Rev.* E **62** 2493

[33] von Grünberg H H 2000 *J. Phys.: Condens. Matter* **12** 6039

[34] Leote de Carvalho R J F, Trizac E and Hansen J-P 1998 *Europhys. Lett.* **43** 369

[35] Alfrey T, Berg P and Morawetz H J 1951 *J. Polym. Sci.* **7** 543

Fuoss R M, Katchalsky A and Lipson S 1951 *Proc. Natl Acad. Sci. USA* **37** 579
le Bret M and Zimm B H 1984 *Biopolymers* **23** 287
[36] Metropolis N, Rosenbluth A W, Rosenbluth M N, Teller A N and Teller E 1953 *J. Chem. Phys.* **21** 1087
[37] Allen M P and Tildesley D J 1987 *Computer Simulation of Liquids* (Oxford: Clarendon)
[38] Frankel D and Smit B 1996 *Understanding Molecular Simulation* (London: Academic)
[39] Marcus R A 1955 *J. Chem. Phys.* **23** 1057
[40] Durand E 1966 *Electrostatique* vol 3 (Paris: Masson) p 230